



TITLE:

Optimization of electrolysis conditions for ti film electrodeposition from lif-licl eutectic molten salt

AUTHOR(S):

Unoki, Makoto; Norikawa, Yutaro; Yasuda, Kouji; Nohira, Toshiyuki

CITATION:

Unoki, Makoto ...[et al]. Optimization of electrolysis conditions for ti film electrodeposition from lif-licl eutectic molten salt. ECS Transactions 2020, 98(10): 393-400

ISSUE DATE:

2020

URL:

<http://hdl.handle.net/2433/255865>

RIGHT:

This is the Accepted Manuscript version of an article accepted for publication in ECS Transactions. The Electrochemical Society and IOP Publishing Ltd are not responsible for any errors or omissions in this version of the manuscript or any version derived from it. The Version of Record is available online at <https://doi.org/10.1149/09810.0393ecst>.; この論文は出版社版ではありません。引用の際には出版社版をご確認ご利用ください。; This is not the published version. Please cite only the published version.

Optimization of Electrolysis Conditions for Ti Film Electrodeposition from LiF–LiCl Eutectic Molten Salt

Makoto Unoki^a, Yutaro Norikawa^a, Kouji Yasuda^{b,c,*}, and Toshiyuki Nohira^a

^a Institute of Advanced Energy, Kyoto University, Uji 611-0011, Japan

^b Agency for Health, Safety and Environment, Kyoto University, Kyoto 606-8501, Japan

^c Graduate School of Energy Science, Kyoto University, Kyoto 606-8501, Japan

* Present address: Graduate School of Engineering, Kyoto University, Kyoto 606-8501, Japan

The optimum conditions for electrodeposition of compact, smooth and adherent Ti films in LiF–LiCl–Li₃TiF₆ at 823 K were investigated. The Li₃TiF₆ was formed in situ in the melt via comproportionation reaction between Li₂TiF₆ and Ti powder. The solubility of Li₃TiF₆ was confirmed to be higher than 7.1 mol% by cyclic voltammetry and ICP-AES measurement. Galvanostatic electrolysis was conducted on Ni plate substrates at various concentrations of Li₃TiF₆ (0.55, 2.6, 7.1 mol%) and cathodic current density (50–1200 mA cm⁻²). Ti films with smoother surface were obtained at higher Li₃TiF₆ concentration and lower current density. In the present study, the smoothest surface Ti films were obtained at 7.1 mol% of Li₃TiF₆ and 50 mA cm⁻² of cathodic current density.

Introduction

Titanium is a metal having excellent properties such as high specific strength, high corrosion resistance and high biocompatibility. Therefore, titanium is utilized for aircraft components, chemical plants, medical components, etc. Furthermore, titanium is attractive metal in terms of its abundant resources. However, widespread use of titanium is prevented due to the high smelting cost and the poor workability. As a method to solve these problems, titanium plating is an attractive technique because superior surface properties of titanium can be utilized. Among titanium plating methods, electrolytic plating is a promising candidate because of the advantages of higher deposition rate and shape flexibility. Electrodeposition of titanium has been studied using aqueous solutions (1,2), organic solvents (3,4), and high-temperature molten salts (5–13) as electrolytes. Nevertheless, pure titanium can be electrodeposited only from high-temperature molten salts.

In previous studies, chlorides (5–7), fluorides (8–10), and fluoride-chloride mixtures (11–13) have been mainly used as molten salt electrolytes. Generally, fluoride molten salts are advantageous for electrodepositing compact and smooth titanium films. Robin *et al.* obtained comparatively compact and smooth films in LiF–NaF–KF melts at 873–923 K (9). In the case of fluoride-chloride mixtures, several researchers reported that Ti films having better morphology can be obtained from the melts with sufficient fluoride concentrations. Takamura *et al.* reported that the morphology of deposits was improved by adding LiF to LiCl–KCl at 773 K (7). Song *et al.* reported that Ti metal with fine crystal grains was obtained when KF was added to NaCl–KCl at 1073 K (13). Based on these reports, we have focused on the electrodeposition of titanium in fluoride-chloride mixtures

consisting of single cations and having enough fluoride concentrations (14–17). We have already reported the electrochemical behaviors of Ti(III) ions and the electrodeposition of Ti in molten KF–KCl (45:55 mol%, 923 K) (14–16) and LiF–LiCl (45:55 mol%, 923 K) (17). We found that LiF–LiCl has an advantage for electrodepositing smooth Ti films due to its lower melting point (774 K at the eutectic composition (18)). In general, smoother Ti films are expected to be obtained at lower temperature by suppressing the growth of crystal grains. Thus, LiF–LiCl eutectic molten salt was selected to obtain Ti films with smooth surface.

In this study, we investigated the effect of Li_3TiF_6 concentration and current density on the morphology of electrodeposited Ti in LiF–LiCl eutectic molten salt at 823 K. First, the solubility of Li_3TiF_6 was investigated by cyclic voltammetry and inductive coupled plasma-atomic emission spectroscopy (ICP-AES) measurement. Second, galvanostatic electrolysis was conducted at various current densities at three different concentrations of Li_3TiF_6 (0.55, 2.6, 7.1 mol%). The optimum conditions to obtain compact and smooth Ti films were evaluated by scanning electron microscopy (SEM), surface roughness (S_a), and X-ray diffraction (XRD) measurement.

Experimental

Reagent-grade LiF (FUJIFILM Wako Pure Chemical Corp., >98.0%) and LiCl (FUJIFILM Wako Pure Chemical Corp., >99.0%) were separately dried under vacuum at 453 K for over 24 h. They are further dried under vacuum at 773 K for 24 h. The salts were mixed in the eutectic composition (molar ratio of LiF:LiCl = 30:70, melting point = 774 K (18), 300 g) and loaded in a graphite crucible (Toyo Tanso Co., Ltd., outer diameter: 90 mm, inner diameter: 80 mm, and height: 120 mm) or a Ni crucible (Chiyoda Industry Manufacturing Plant Co., Ltd., outer diameter: 98 mm, inner diameter: 96 mm, height: 102 mm). The mixture in the crucible was placed at the bottom of a stainless-steel vessel in an airtight Kanthal container. The electrochemical measurements were conducted in dry Ar atmosphere at 823 K in a glove box. After blank measurements in molten LiF–LiCl, 0.50–5.0 mol% of Li_2TiF_6 and 0.33–3.3 mol% of Ti powder (Kojundo Chemical Laboratory Co., Ltd., 99.9%) were added to the melt. Here, the synthetic method of Li_2TiF_6 was reported in our previous paper (17). The added amounts of Ti powder were approximately twice the amounts necessary to generate Ti(III) ions by comproportionation reaction between Ti(IV) ions and Ti(0) according to Eq. 1.



This reaction is also described as:



Electrochemical measurements and galvanostatic electrolysis were conducted using a three-electrode method with an electrochemical measurement system (Hokuto Denko

Corp., HZ-7000). The working electrodes were Ni plate (Nilaco Corp., 10 mm × 10 mm, thickness: 0.1 mm, 99.95%), Mo flag (Nilaco Corp., diameter: 3.0 mm, thickness: 0.1 mm, 99.95%), Au flag (Nilaco Corp., diameter: 3.0 mm, thickness: 0.1 mm, 99.98%), and glass-like carbon rod (Tokai Carbon Co., Ltd., diameter: 3.0 mm) electrodes. The structure of the flag electrodes was reported in our previous paper (19). Ti rods (Nilaco Corp., diameter: 3.0 mm, 99.5%) were used as the counter and reference electrodes. In the blank measurement, a Pt wire (Nilaco Corp., diameter: 1.0 mm, 99.98%) was used as the quasi-reference electrode. The potential of reference electrodes was calibrated with respect to a dynamic Cl_2/Cl^- potential determined by cyclic voltammetry on a glass-like carbon rod electrode. The melt temperature was measured using a type-K thermocouple. The electrolyzed samples on the Ni plates were soaked in distilled water for 30 min and $\text{Al}(\text{NO}_3)_3$ aqueous solution (1.0 mol L^{-1} , obtained from FUJIFILM Wako Pure Chemical Co., Ltd., 98.0%) for 10 min at room temperature to remove the salt adhered on the deposits.

The surface and cross-section of the samples were observed by using scanning electron microscopy (SEM; Thermo Fisher Scientific Inc., Phenom Pro Generation 5). Before the observation of the cross section, the samples were cut at the center and embedded in acrylic resin. The samples were polished with emery papers, buffing compounds and a cross-section polisher (CP; Hitachi, Ltd., IM4000). The samples were then coated with Au using an ion-sputtering apparatus (Hitachi, Ltd., E-1010) to impart conductivity. The surface roughness (S_a) of the samples was also measured by SEM and calculated as the average of 5 points (the measurement conditions: shortest cut-off $\lambda_s = 20 \text{ nm}$, longest cut-off $\lambda_c = 240 \mu\text{m}$, measured area $A = 1.2 \times 1.2 \text{ mm}$). The samples were also characterized by energy-dispersive X-ray spectroscopy (EDX; Thermo Fisher Scientific Inc., Phenom Pro Generation 5) and X-ray diffraction (XRD; Rigaku Corp., Ultima IV, Cu- $K\alpha$ line). A small portion of the molten salt was sampled by the suction method using a borosilicate glass tube (Pyrex®, outer diameter: 6 mm, inner diameter: 4 mm) and dissolved in HNO_3 aqueous solution (pH 1, obtained from Tama Chemical Corp., AA-100 grade, 68 wt%). The solution was analyzed by using inductive coupled plasma-atomic emission spectroscopy (ICP-AES; Hitachi, Ltd., SPECTRO BLUE) to determine the concentration of Li_3TiF_6 in the sampled molten salt.

Result and discussion

In-situ preparation of Li_3TiF_6

Prior to electrodeposition, the solubility of Li_3TiF_6 was investigated with cyclic voltammetry and ICP-AES measurement. As described in Eq. 2, the Li_3TiF_6 are synthesized in the molten LiF-LiCl via the comproportionation reaction between Li_2TiF_6 and Ti powder.

Figure 1 (a) shows the cyclic voltammogram at a Au flag electrode in the positive potential region after the addition of Li_2TiF_6 (0.50–5.0 mol%) and Ti powder (0.33–3.3 mol%). The redox currents of Ti(III)/Ti(IV) were observed around $-0.8 \text{ V vs. Cl}_2/\text{Cl}^-$ at each added amount of Li_2TiF_6 . Figure 1 (b) shows the plots of peak current densities of each cyclic voltammogram against the added amounts of Li_2TiF_6 . The peak current densities increased almost linearly as the Li_2TiF_6 was added. This result indicates that the

added Li_2TiF_6 were almost completely dissolved up to 5.0 mol% to form Ti(III) ions by the comproportionation reaction.

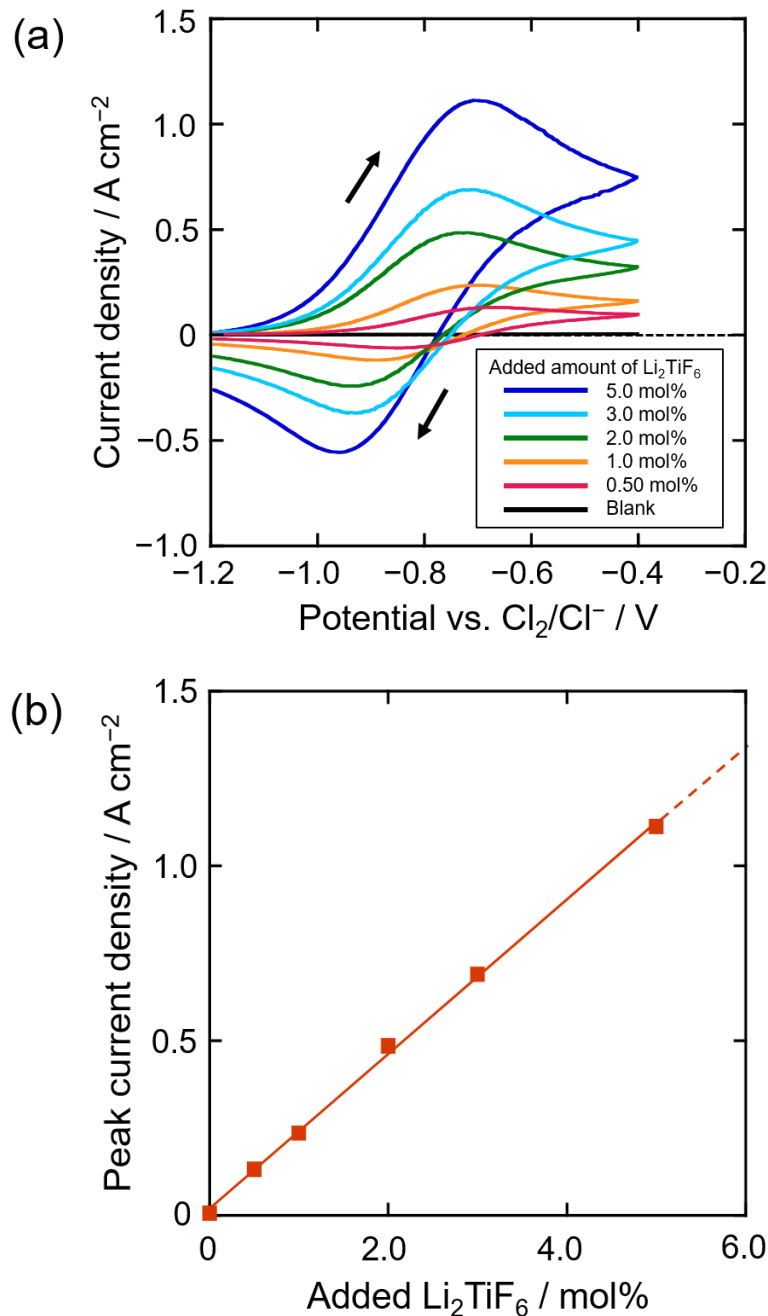


Figure 1. (a) Cyclic voltammograms at a Au flag electrode in molten LiF–LiCl after adding various amounts of Li_2TiF_6 (0–5.0 mol%) and Ti powder (0–3.3 mol%) at 823 K. Scan rate: 0.50 V s^{-1} . (b) Dependence of anodic peak current density on added amount of Li_2TiF_6 .

Figure 2 shows the plots of the concentrations of Li_3TiF_6 determined by ICP-AES measurement against the added amounts of Li_2TiF_6 . The black solid line indicates the theoretical value calculated from Eq. 2 and the red dots are the measured values. In this study, the concentration of Li_3TiF_6 is defined by the following equation.

$$[\text{Li}_3\text{TiF}_6] = n_{\text{Li}_3\text{TiF}_6} / (n_{\text{LiF}} + n_{\text{LiCl}} + n_{\text{Li}_3\text{TiF}_6}) \quad [3]$$

Here, $n_{\text{Li}_3\text{TiF}_6}$, n_{LiF} and n_{LiCl} indicate the molar amounts of Li_3TiF_6 , LiF and LiCl in the molten salt, respectively. Since LiF is consumed in the comproportionation reaction of Eq. 2, the theoretical concentrations of Li_3TiF_6 are not simply four-thirds of the added amounts of Li_2TiF_6 . Therefore, the theoretical value is not completely linear to the added amounts of Li_2TiF_6 . As shown in Figure 2, the measured values were close to the theoretical ones up to 7.1 mol% of Li_3TiF_6 . Thus, the solubility of Li_3TiF_6 is confirmed to be more than 7.1 mol%.

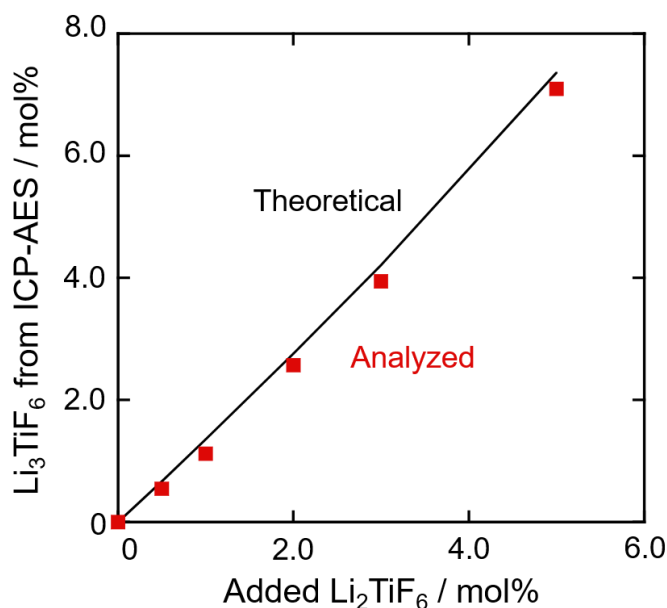


Figure 2. The concentration of Li_3TiF_6 determined by ICP-AES in molten LiF-LiCl after adding various amounts of Li_2TiF_6 (0–5.0 mol%) and Ti powder (0–3.3 mol%) at 823 K.

Electrodeposition of Ti films

Galvanostatic electrolysis at Ni plate substrates was conducted under the conditions of various current densities ($50\text{--}1200 \text{ mA cm}^{-2}$) and Li_3TiF_6 concentrations (0.55, 2.6, 7.1 mol%). Here, the reduction current is expressed as a positive value. The electric charge density was fixed at 60 C cm^{-2} for all electrolysis. The theoretical thickness of electrodeposited Ti films at 60 C cm^{-2} is $22 \text{ }\mu\text{m}$. Figure 3 shows optical images of the electrodeposited samples after washing with distilled water and $1 \text{ mol L}^{-1} \text{ Al}(\text{NO}_3)_3$ aqueous solution. XRD measurement confirmed that the electrodeposits were Ti . Compact and highly adherent Ti films were obtained at all Li_3TiF_6 concentrations at 50 mA cm^{-2} . As the concentration is increased, Ti films can be obtained even at higher current densities; Ti films were obtained up to 200 mA cm^{-2} at 2.6 mol% of Li_2TiF_6 and up to 400 mA cm^{-2} at 7.1 mol%. On the other hand, the morphology of the deposits changed to powder-like as

the current densities further increased; the powder-like deposits were obtained at higher current density than 400 mA cm^{-2} at 2.6 mol% and higher than 800 mA cm^{-2} at 7.1 mol%.

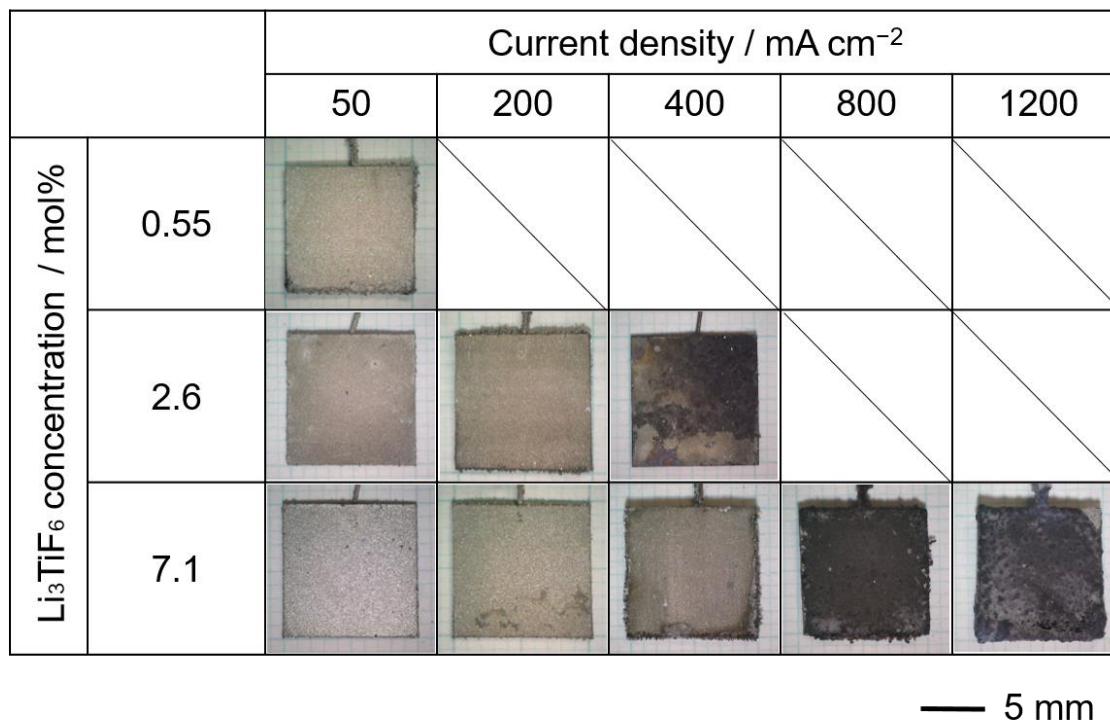


Figure 3. Optical images of the samples obtained by galvanostatic electrolysis at Ni plates in molten LiF–LiCl–Li₃TiF₆ at 823 K. Charge density: 60 C cm^{-2} .

Figure 4 compares the surface/cross-sectional SEM images and surface roughness (S_a) at the same current density (50 mA cm^{-2}) at various Li₃TiF₆ concentrations. The formation of compact and adherent Ti film was also confirmed by the SEM images. The smoothness of the deposits was improved as the Li₃TiF₆ concentration increased. The smallest S_a ($1.32 \text{ }\mu\text{m}$), which means the smoothest surface, was obtained at 7.1 mol% of Li₃TiF₆.

Figure 5 shows the surface/cross-sectional SEM images and surface roughness (S_a) at the same Li₃TiF₆ concentration (7.1 mol%) at various current densities. In the case of at 400 mA cm^{-2} , the compactness and adhesion were almost the same as those of 50 mA cm^{-2} . However, the roughness was increased and nodule electrodeposits were partially observed. At a very high current density of 1200 mA cm^{-2} , the morphology of electrodeposits was powder-like and the adhesion was quite low.

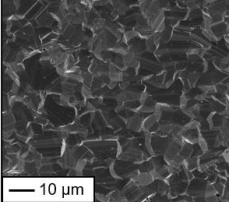
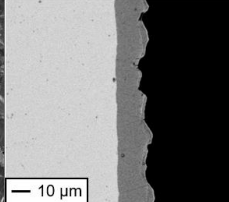
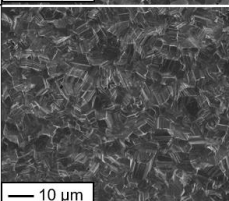
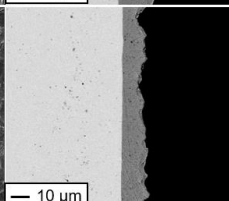
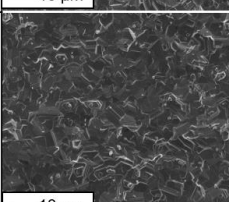
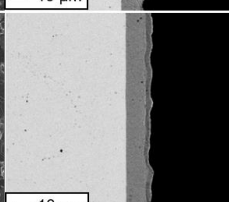
		Surface	Cross-section	S_a (μm)
Li ₃ TiF ₆ concentration / mol%	0.55			2.04
	2.6			2.17
	7.1			1.32

Figure 4. Surface/cross-sectional SEM images and surface roughness (S_a) of the samples obtained by galvanostatic electrolysis at Ni plates in LiF–LiCl–Li₃TiF₆ at 823 K. Charge density: 60 C cm⁻². Current density: 50 mA cm⁻².

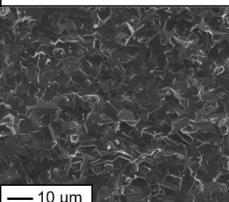
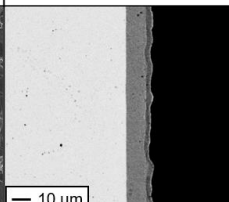
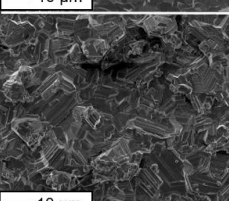
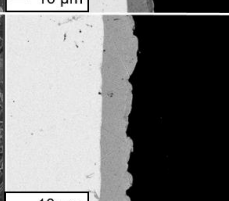
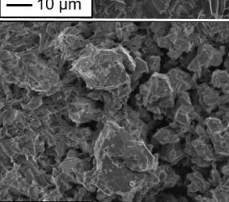
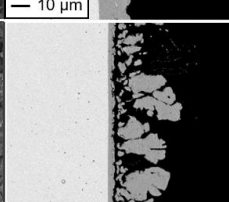
		Surface	Cross-section	S_a (μm)
Current density / mA cm ⁻²	50			1.32
	400			2.83
	1200			—

Figure 5. Surface/cross-sectional SEM images and surface roughness (S_a) of the samples obtained by galvanostatic electrolysis at Ni plates in LiF–LiCl–Li₃TiF₆ at 823 K. Charge density: 60 C cm⁻². Li₃TiF₆ concentration: 7.1 mol%.

Conclusion

The optimum conditions for electrodepositing compact, smooth and adherent Ti films were investigated in LiF–LiCl–Li₃TiF₆ at 823 K. The solubility of Li₃TiF₆ was confirmed to be more than 7.1 mol% by cyclic voltammetry and ICP-AES measurement. Galvanostatic electrolysis was conducted on Ni plate substrates at various Li₃TiF₆ concentrations (0.55, 2.6, 7.1 mol%) and current densities (50–1200 mA cm⁻²). As a result, Ti films with smoother surface was obtained at higher Li₃TiF₆ concentration and lower current density. In the present electrolysis conditions, the smoothest surface Ti films were obtained at 7.1 mol% of Li₃TiF₆ and 50 mA cm⁻².

Acknowledgments

A part of this study was conducted as a collaborative research with Sumitomo Electric Industries, Ltd.

References

1. S. Morioka and A. Umezono, *J. Jpn. Inst. Metals.*, **23**, 71 (1959).
2. S. Kazuo and A. Kitani, *Electrochemistry*, **52**, 302 (1984).
3. S. Biallozor and A. Lisowska, *Electrochim. Acta*, **25**, 1209 (1980).
4. A. Lisowska and S. Biallozor, *Electrochim. Acta*, **27**, 105 (1982).
5. M. B. Alpert, F. J. Schultz, and W. F. Sullivan, *J. Electrochem. Soc.*, **104**, 555 (1957).
6. G. M. Haarberg, W. Rolland, A. Sterten, and J. Thonstad, *J. Appl. Electrochem.*, **23**, 217 (1993).
7. H. Takamura, I. Ohno, and H. Numata, *J. Jpn. Inst. Metals*, **60**, 388 (1996).
8. J. De Lepinay, J. Bouteillon, S. Traore, D. Renaud, and M. J. Barbier, *J. Appl. Electrochem.*, **17**, 294 (1987).
9. A. Robin, J. De Lepinay, and M. J. Barbier, *J. Electroanal. Chem.*, **230**, 125 (1987).
10. M. E. Sibert and M. A. Steinberg, *J. Electrochem. Soc.*, **102**, 641 (1955).
11. D. Wei, M. Okido, and T. Oki, *J. Appl. Electrochem.*, **24**, 923 (1994).
12. V. V. Malyshev and D. B. Shakhnin, *Mater. Sci.*, **50**, 80 (2014).
13. J. Song, Q. Wang, X. Zhu, J. Hou, S. Jiao, and H. Zhu, *Mater. Trans.*, **55**, 1299 (2014).
14. Y. Norikawa, K. Yasuda, and T. Nohira, *Mater. Trans.*, **58**, 390 (2017).
15. Y. Norikawa, K. Yasuda, and T. Nohira, *Electrochemistry*, **86**, 99 (2018).
16. Y. Norikawa, K. Yasuda, and T. Nohira, *J. Electrochem. Soc.*, **166**, D755 (2019).
17. Y. Norikawa, K. Yasuda, and T. Nohira, *J. Electrochem. Soc.*, **167**, 082502 (2020).
18. J. Sangster and A. D. Pelton, *J. Phys. Chem. Ref. Data*, **16**, 509 (1987).
19. K. Maeda, K. Yasuda, T. Nohira, R. Hagiwara, and T. Homma, *J. Electrochem. Soc.*, **162**, D444 (2015).